13

Centennial-to-millennial-scale Holocene climate variability in the North Atlantic region induced by noise

MATTHIAS PRANGE, JOCHEM I. JONGMA AND MICHAEL SCHULZ

Under pre-industrial Holocene boundary conditions, a three-dimensional global climate model of intermediate complexity exhibits centennial-to-millennial-scale climate variability in the North Atlantic. The climate variability is associated with noise-induced 'on' and 'off' switches in Labrador Sea convection. On a multicentennial time scale these stochastic mode-transitions can be phase-locked to a small periodic freshwater forcing. These results suggest a stochastic resonance mechanism that can operate under Holocene conditions, involving changes in North Atlantic Deep Water formation as an important amplifying mechanism of relatively weak climate perturbations. We introduce a conceptual nonlinear stochastic model that reproduces the noise-induced transitions and highlights the importance of polar water flow towards the Labrador Sea in setting the stochastic time scale. Moreover, we present a new hypothesis in an attempt to explain an observed mid-Holocene mode shift in the power spectrum of North Atlantic climate variability from ~1500 to 600–1000 years. This hypothesis involves a mid-Holocene increase of polar water flow from the Greenland Sea into the Labrador Sea. The resulting decrease of the stochastic time scale favours the phase-locking to a smaller period in an applied multimodal external forcing, in accordance with stochastic resonance theory.

13.1 Introduction

Even though the climate of the Holocene (i.e. the past ~10 000 years) is generally regarded to be stable compared to the strongly fluctuating climate of the last ice age, a number of studies have revealed substantial Holocene climate variations in the North Atlantic at time scales ranging from centuries to a few millennia (e.g. O'Brien *et al.* 1995; Bond *et al.* 1997, 2001; Bianchi & McCave 1999; Schulz &

Paul 2002; Hall *et al.* 2004). The causes of these climate variations remain a source of debate. Hypotheses regarding their origin include internal oscillations of the climate system (e.g. Schulz & Paul 2002), external forces like variations in the Sun's radiative output (e.g. Bond *et al.* 2001) and/or a combination of the two. Based on analogies to larger-amplitude climate variations and proxy evidence, many authors have concluded that the Holocene climate fluctuations at centennial-to-millennial time scales, specifically those reconstructed for the North Atlantic region, are linked to variations in the rate of North Atlantic Deep Water (NADW) formation and associated changes in the Atlantic meridional overturning circulation (AMOC) and the oceanic northward heat transport (e.g. Bond *et al.* 2001; Oppo *et al.* 2003).

Recently, Berner *et al.* (2008) produced a new subpolar sea-surface temperature (SST) record with very high temporal resolution that provides new insights into Holocene climate variability in the North Atlantic. The record reveals Holocene multicentennial-to-millennial-scale SST variability on the order of 1–3° C southwest of Iceland. Climatic oscillations (note that we use the term 'oscillation' without implying strict periodicity) with 600- to 1000-, ~1500- and 2500-year periods are documented, with a time-dependent dominance of different periods through the Holocene. In the mid Holocene (7000–5000 years ago) a mode shift in the variability from higher (~1500 years) to lower (600–1000 years) periods is observed. Another important feature of the subpolar SST record is its correlation with reconstructed solar irradiance variability. So far, a theory for the centennial-to-millennial-scale North Atlantic climate variability, which accounts for both the relation to solar irradiance and the mid-Holocene shift in the power spectrum towards smaller periods, is lacking.

Based on results obtained with a global atmosphere–ocean model of intermediate complexity (Schulz *et al.* 2007; Jongma *et al.* 2007) we shall develop a conceptual model that may help to understand Holocene climate variability in the North Atlantic. The conceptual model involves noise-induced transitions between different states of the AMOC and a stochastic resonance mechanism to explain the subpolar SST record.

13.2 North Atlantic climate variability in an intermediate-complexity atmosphere–ocean model

To examine the potential of the climate system to generate centennial-to-millennial-scale oscillations, Schulz *et al.* (2007) used the global three-dimensional atmosphere–ocean model ECBilt-CLIO, version 3. This coupled model of intermediate complexity derives from the atmosphere model ECBilt (Opsteegh *et al.* 1998) and the ocean/sea-ice model CLIO (Goosse & Fichefet 1999). The atmospheric component solves the quasi-geostrophic equations with T21 resolution (~5.6°) for

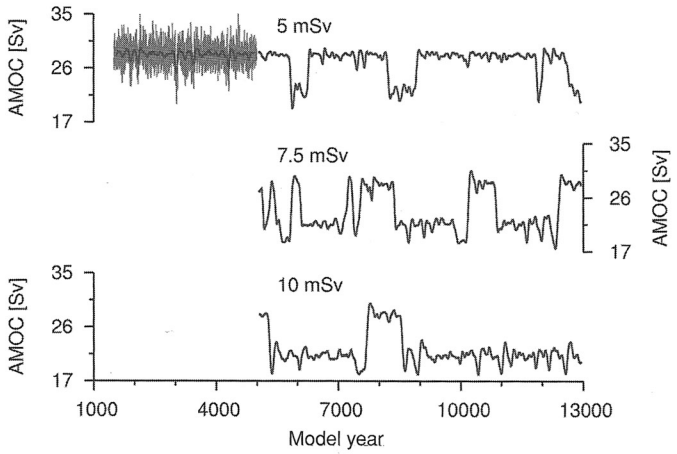

Figure 13.1 Time series of the maximum of the Atlantic meridional overturning circulation (AMOC), calculated north of 30° N and below 500 m water depth in ECBilt–CLIO. (Top) Unsmoothed annual values from the unperturbed control experiment (prior to model year 5000). The corresponding output from a 101-year wide Hanning filter is overlayed. After model year 5000 a 5 mSv freshwater perturbation is applied to the Labrador Sea. The resulting AMOC time series (smoothed) oscillates between approximately 22 and 28 Sv. (Centre) AMOC for a 7.5 mSv freshwater perturbation starting in model year 5000 (smoothed time series). (Bottom) As before, but for a 10 mSv forcing (Schulz *et al.* 2007).

three layers. Variability associated with large-scale weather patterns is explicitly computed. The primitive-equation, free-surface ocean component has a horizontal resolution of 3° and 20 levels in the vertical and uses a rotated subgrid in the North Atlantic Ocean to avoid the convergence of meridians near the north pole. It includes parameterisations for mixed-layer dynamics, downsloping currents and the Gent–McWilliams (1990) parameterisation of subgrid-scale processes. The ocean model is coupled to a thermodynamic–dynamic sea-ice model with viscous-plastic rheology.

For pre-industrial boundary conditions ECBilt-CLIO captures the two main deep convection sites in the modern North Atlantic. Consistent with observations, stable deep convection occurs in the Labrador Sea and in the Nordic seas (Schulz *et al.* 2007). On adding a weak, constant freshwater flux of 5–10 mSv (milli-Sverdrup; 1 Sv = 10^6 m^3s^{-1}) to the surface of the Labrador Sea, the character of the AMOC changes fundamentally (note that the applied freshwater forcings are at least one order of magnitude below the values typically used in 'freshwater-hosing experiments' to yield a complete shut-down of NADW formation). The forcing gives rise to a bimodal AMOC distribution with random timing of transitions between a strong and a weak overturning state (Fig. 13.1). Transitions between the

strong state and the weak state are related to 'on' and 'off' switches in Labrador Sea convection, while NADW formation in the Nordic seas remains nearly unaffected. With increasing magnitude of the freshwater forcing the probability for the system to occupy the weak state rises.

In the experiments of Schulz *et al.* (2007) the cessation of deep-water formation in the Labrador Sea causes a drop in the temperature of the overlying air by ~3 °C (due to a reduced oceanic heat transport by the AMOC towards that region), consistent with the Holocene multicentennial-to-millennial-scale SST variability reconstructed by Berner *et al.* (2008). This temperature anomaly spreads over southern Greenland in the model, while air temperatures over central Greenland remain virtually unaffected. Indeed, it has long been recognised that temperature reconstructions from central Greenland show only little variability during the Holocene (specifically, if compared to the last glacial period; e.g. Grootes & Stuiver 1997). The ECBilt-CLIO model results suggests that larger temperature variations can be expected to be documented in southern Greenland, which is in agreement with palaeoclimatic evidence from borehole records (Dahl-Jensen *et al.* 1998).

The duration between subsequent 'on'/'off' switches in Labrador Sea convection and hence AMOC mode-transitions varies widely from 310 to 2660 years in the 7.5 mSv experiment (Fig. 13.1). The average duration is approximately 1420 years and the standard deviation amounts to 1020 years. Hence, the total range of values is almost completely covered by the interval of one standard deviation around the mean, supporting the notion that the durations are more or less uniformly distributed. The lack of a dominant time scale argues against a deterministic process controlling the timing of the AMOC oscillations and is easier to reconcile with a stochastic origin (note that we use the term 'stochastic' in a somewhat loose sense – in the coupled climate model any 'randomness' is generated by the interactions of deterministic processes which lead to high-frequency noise). Therefore, the simplest explanation for the AMOC oscillations involves a bistable system with noise-induced transitions from one mode of operation to the other.

Bistability of the system can be understood by means of a positive feedback between oceanic salt transport and Labrador Sea convection, according to the well-known 'Stommel feedback' (Stommel 1961). The NADW formation in the Labrador Sea drives a part of the AMOC which, in turn, transports salt from the subtropics towards the subpolar convective site. This salt supply (together with heat loss to the atmosphere) maintains a high density of surface waters and hence convection (this is the 'on' mode). A disruption of this 'conveyor belt' (e.g. by a randomly occuring negative density perturbation in the Labrador Sea) will result in a freshening of Labrador Sea surface water (due to excess precipitation and runoff) and may eventually lead to a halt of convection ('off' mode).

Given the noise-induced transitions between the states with and without convection in the Labrador Sea, the change in the ratio of the durations of the strong state to the weak state of the AMOC oscillations (cf. Fig. 13.1) can be explained. Starting from a strong state, a larger value of the continuous freshwater forcing brings the Labrador Sea closer to the point at which a random negative density anomaly can stop the deep mixing. Thus, the probability for a shut-down of convection in the Labrador Sea increases with increasing freshwater forcing. Once the system is in the weak mode, the likelihood for a large positive density anomaly determines how long this mode prevails. Since a larger freshwater forcing moves the Labrador Sea towards less dense surface waters, the probability for a weak-to-strong transition decreases with increasing freshwater forcing.

Even though the oscillations produced by ECBilt-CLIO might provide an explanation for Holocene centennial-to-millennial-scale variability in the North Atlantic, this explanation would not account for the phase-locking to the Sun's activity that has been suggested in previous studies (Bond *et al.* 1997, 2001; Berner *et al.* 2008). Jongma *et al.* (2007), however, have shown that the transitions between the two modes of the AMOC can be phase-locked to a small multicentennial periodic forcing.

13.3 Synchronisation with an external forcing

North Atlantic drift-ice and SST proxies correlate with reconstructed production rates of cosmogenic isotopes, which has been taken as evidence of a persistent solar influence on Holocene high-latitude climate (Bond *et al.* 1997, 2001; Berner *et al.* 2008). However, the direct effect of solar irradiance variations is considered too small to explain the observed climate variability in the Holocene (e.g. Rind 2002). Accordingly, an amplifying mechanism is required to explain centennial-to-millennial Holocene climate variability driven by a solar forcing. Jongma *et al.* (2007) demonstrated that changes in the NADW production rate can provide an amplifying mechanism of relatively weak climate perturbations during the Holocene – a mechanism that had previously been hypothesised by Bond *et al.* (2001).

To investigate whether ECBilt-CLIO's AMOC oscillations are susceptible to small external forcings, a periodically varying freshwater forcing was applied to the Labrador Sea instead of a constant one (Jongma *et al.* 2007). This freshwater flux varied sinusoidally between 5 and 10 mSv with a period of 500 years (the exact choice of the forcing period was not important; the authors just wanted to test whether the AMOC oscillations could be phase-locked to a *centennial-to-millennial-scale* forcing). It is important to realise that the amplitude of the forcing is sufficiently small to keep the system always in the bimodal regime (Fig. 13.1).

Accordingly, the periodic forcing was considered 'small' (or sub-threshold) since noise is required to trigger individual state switches.

In a 12 000-year long integration of ECBilt-CLIO, Jongma *et al.* (2007) found 10 AMOC state transitions to the weak mode (i.e. Labrador Sea convection 'off'-switches). A Rayleigh test showed that the timing of the mode-transitions was significantly ($p < 0.05$) phase-locked to the periodic forcing. Accordingly, the response of the system to the forcing occured approximately at integer multiples of the forcing period.

Intuitively, noise might be expected to weaken or obscure regular signals. However, in a bistable system the presence of noise can provide a crucial mechanism for the system to explore its possible states (Nicolis & Nicolis 1981). Consequently, the timing of the state switches in the experiment of Jongma *et al.* (2007) has a stochastic component. The response of the AMOC to the periodic forcing is both deterministic and stochastic, i.e. 'quasi-deterministic' (Freidlin & Wentzell 1998).

Noise-assisted amplification of a small periodic forcing is a stochastic resonance phenomenon (Benzi *et al.* 1981; Gammaitoni *et al.* 1998). It has been shown that on an 'interval of resonance' (a set of scale parameters for which chaotic or trivial behaviour of the system is excluded), there must exist a stochastic resonance point (Herrmann & Imkeller, 2005). The lower limit of this interval of resonance, below which the system remains practically in one of the states, coincides with a minimum exponential time scale for quasi-deterministic behaviour (Freidlin & Wentzell 1998; Freidlin 2000). The upper limit of this interval refers to a situation where the system switches chaotically between multiple states. By showing prolonged but finite noise-induced mode transitions that are significantly deterministic, Jongma *et al.* (2007) argued that the modelled climate system operates on this interval of resonance, implying that a stochastic resonance mechanism can be operational with respect to centennial-to-millennial North Atlantic climate variability in the Holocene. (Note that finding the stochastic resonance point, i.e. the time scale at which the system response is maximum, was not the authors' intention.)

13.4 A conceptual model of North Atlantic climate oscillations

Probably the simplest model that captures the *basic* mechanisms of the centennial-to-millennial-scale oscillations consists of two prognostic variables, θ and S, representing spatially averaged temperature and salinity of the upper (say, the topmost 200 m) Labrador Sea (Schulz *et al.* 2007). Hydrographic conditions in the upper Labrador Sea depend on the wind- and density-driven inflows from the subtropical Atlantic, the influx of polar water from the Greenland Sea (via the East Greenland Current through Denmark Strait) and surface fluxes. The deterministic governing

equations for Labrador Sea temperature and salinity can therefore be formulated as

$$\frac{dS}{dt} = \frac{1}{V}[(q_1+\phi)S_1 + q_2S_2 - (q_1 + q_2 + \phi + P + P')S], \tag{13.1}$$

$$\frac{d\theta}{dt} = \frac{1}{V}[(q_1 + \phi)\theta_1 + q_2\theta_2 - (q_1 + q_2 + \phi)\theta] + H, \tag{13.2}$$

where V denotes the volume of the upper Labrador Sea (3×10^{14} m^3), q_1 is the wind-driven volume flux from the subtropical Atlantic, ϕ is the density-driven (overturning) volume flux from the subtropical Atlantic, q_2 is the volume flux from the Greenland Sea, P denotes a basic surface freshwater flux into the Labrador Sea (78 mSv), P' is a freshwater flux perturbation, H denotes the surface heat flux and t is time. The parameters S_1, θ_1 and S_2, θ_2 denote salinities and temperatures of the inflowing subtropical and polar water masses, respectively. To keep the model as simple as possible, the wind-driven volume fluxes are assumed to be constant ($q_1 =$ 2 Sv, $q_2 = 2$ Sv; after Fig. 10.50 in Dietrich *et al.* 1975). Likewise, any temperature and salinity changes in the water masses originating from the subtropical Atlantic and the Greenland Sea are neglected ($S_1 = 35.3$ psu, $\theta_1 = 8\,°$C, $S_2 = 34.6$ psu, $\theta_2 = 1.5\,°$C). The overturning ϕ couples the pair of differential equations through a linear dependence on the density difference between the Labrador Sea and the subtropical Atlantic, i.e. $\phi = \kappa[\alpha\ (\theta_1 - \theta) - \beta\ (S_1 - S)]$, where α and β denote the thermal and haline expansion coefficients of seawater ($\alpha = 0.1$ K^{-1}, $\beta =$ 0.8 psu^{-1}). The tuning parameter κ is set to 70 Sv. If ϕ becomes lower than zero, ϕ is set to zero (Labrador Sea convection 'off'). For the surface heat flux H, a simple restoring term is used, i.e. $H = (\theta_r - \theta)/\tau$, where $\theta_r = 0\,°$C is a relaxation temperature and $\tau = 1$ year is the relaxation time scale. This simple approach parameterises the damping of surface temperature anomalies by atmospheric heat advection and/or longwave radiation.

The stability behaviour of the simple deterministic model is illustrated by the calculation of an equilibrium hysteresis with respect to surface freshwater forcing. The 'Stommel feedback' along with the competition between thermal and saline forcings of the overturning results in multiple equilibria. Plotting the overturning ϕ against the anomalous freshwater forcing P' reveals a regime of bistability for intermediate forcing amplitudes (Fig. 13.2). With $P' = 0$ Sv, for instance, one stable equilibrium ('off' mode) has zero overturning and a Labrador Sea salinity of $S \cong 34.3$ psu, while the other stable equilibrium ('on' mode) yields an overturning of $\phi = 10$ Sv and a salinity of ~35.0 psu. For very large positive/negative values of P', only the 'off'/'on' mode of Labrador Sea overturning provides a stable solution. Since the inflow of polar water ($S_2 = 34.6$ psu) has a higher/lower salinity than the Labrador Sea in the 'off'/'on' mode, it will always counteract the current state

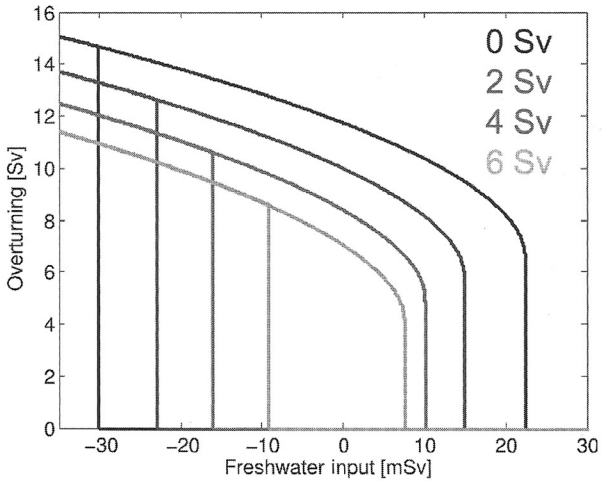

Figure 13.2 Equilibrium hysteresis loops (Labrador Sea overturning ϕ vs. freshwater input P') for the deterministic conceptual model with different values for the polar water inflow to the Labrador Sea ($q_2 = 0$ Sv, 2 Sv, 4 Sv, 6 Sv). The hysteresis loops have been obtained by slowly varying the freshwater input to the Labrador Sea (in the 'clockwise' direction).

of overturning in the Labrador Sea. To demonstrate this, we calculate hysteresis curves for different q_2 (Fig. 13.2). With increasing polar inflow, the hysteresis loop becomes narrower, i.e. smaller positive or negative freshwater perturbations P' are sufficient to induce a transition from one mode to the other. For $q_2 > 13$ Sv the hysteresis disappears and the system becomes monostable (not shown).

The simple deterministic model possesses no internal variability. In the bistable regime of ocean circulation, however, occasional state transitions can be introduced by a stochastic forcing component (cf. Cessi 1994). We add a term $\sigma \xi S_0/V$ to equation (13.1) to introduce a stochastic component in the salinity balance, where ξ represents Gaussian 'quasi white noise' with zero mean and unit variance, σ measures the standard deviation of the stochastic forcing and S_0 denotes a reference salinity (35 psu). We note that the stochastic forcing is *not* perfectly white in time due to a non-vanishing autocorrelation that is introduced by the three-day time step of the Euler scheme used to solve the differential equations. This rather simple approach is similar to numerical schemes used in previous studies on stochastically forced thermohaline flows (e.g. Cessi 1994; Monahan 2002). It is still important to realise that stochastic perturbations that are not white in time may yield significantly different results from those that are white (for an in-depth discussion, see e.g. Stastna & Peltier 2007). However, from a physical point of view it is not reasonable to expect the stochastic climate forcing to be a white-noise process and our simple approach can be interpreted as a particular form of fading memory, i.e. the noise

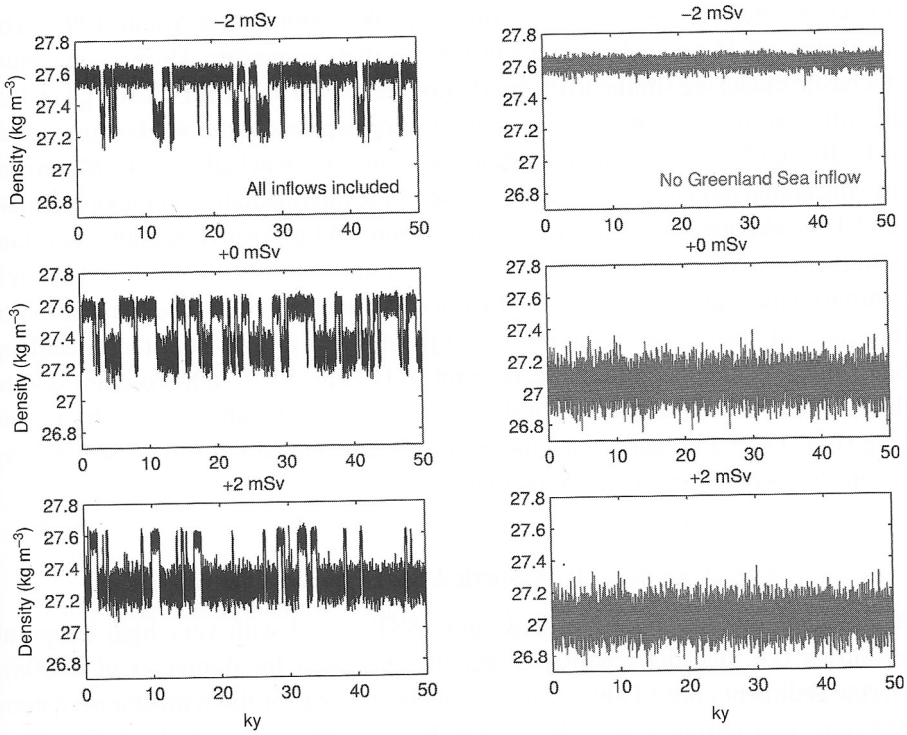

Figure 13.3 Typical time series of Labrador Sea density anomalies in the stochastically forced conceptual model with (left) all inflows included ($q_2 = 2$ Sv) and (right) polar water inflow set to zero ($q_2 = 0$). From top to bottom, the additional constant freshwater influx P' increases from –2 mSv to +2 mSv. Note that time-axis units are 10^3 years, i.e. kiloyears (Schulz *et al.* 2007).

has a perfect memory of three days and then loses all memory (we note that the three-day interval roughly matches the synoptic time scale of the climate system). Therefore, no attempts have been made to solve the stochastic differential equations with a more sophisticated Langevin approach (e.g. Kloeden & Platen 1992) in conjunction with perfectly white noise.

Setting $\sigma = 0.2$ Sv and $q_2 = 2$ Sv, and applying no additional freshwater flux ($P' = 0$ Sv), we obtain numerous transitions from one mode to the other during a 50 000 year integration, resulting in centennial-to-millennial variations of the overturning circulation (Fig. 13.3, left column). The average residence time in a circulation mode before switching back to the other state and, hence, the time scale of the oscillations, depends on the noise intensity (cf. Cessi 1994). The stronger the noise, the larger is the probability for a flip into the other state, and the shorter is the mean residence time in one mode. Note, however, that the underlying bistability of the deterministic system may be completely masked if the amplitude of the

stochastic forcing is too strong (cf. Monahan 2002; Stommel & Young 1993). The value of $\sigma = 0.2$ Sv was chosen such that the oscillations produced by the conceptual stochastic model are similar to the oscillations observed in ECBilt-CLIO (given that the 'off'/'on' mode of the conceptual model corresponds to the weak/strong mode in ECBilt-CLIO, where Labrador Sea convection is switched off/on). Moreover, the conceptual model captures the response of the intermediate-complexity climate model to additional constant freshwater inputs. With positive/negative constant perturbations, the system spends more time in the 'off'/'on' mode (Fig. 13.3, left column), since larger random perturbations are required to induce a transition to the 'on'/'off' mode. In the absence of a polar water inflow from the Greenland Sea ($q_2 = 0$) state transitions become unlikely (Fig. 13.3, right column) due to the different stability behaviour of the system associated with the wider hysteresis loop (Fig. 13.2). In other words, the polar inflow from the Greenland Sea favours stochastic switches from one mode to the other.

13.5 A mode shift in North Atlantic climate variability

A Holocene diatom-based North Atlantic SST record with very high temporal resolution (i.e. decadal-scale) was recently produced by Berner *et al.* (2008). Marine sediment core LO09-14, which has been used for the temperature reconstruction, was retrieved from Reykjanes Ridge southwest of Iceland. The SST record documents climatic oscillations with 600- to 1000-, ~1500-, and 2500-year periodicities, with a time-dependent dominance of different periods through the Holocene. In particular, a striking mode shift is observed during the mid Holocene. Before this shift, the dominant period in SST variability is ~1500 years; after the mode shift, higher-frequency oscillations with a period of 600 to 1000 years prevail. Can such a mode shift be reproduced by our conceptual stochastic model?

To answer this question, we have to discover the processes that determine the time scale of the oscillations in the conceptual model. First and foremost, the average waiting time in one state before switching back to the other state is governed by the noise intensity, as already discussed in the previous section. However, since there is no evidence for a substantial shift in the noise structure over the North Atlantic, we assume a constant noise level throughout the Holocene. Another parameter that is of upmost importance for the time scale of the oscillations is q_2, the volume flux of polar water that flows from the Greenland Sea towards the Labrador Sea. As discussed above, the polar inflow always counteracts the current state of convection in the Labrador Sea and, hence, tends to reduce the width of the equilibrium hysteresis loops, i.e. the regime of bistability. Under a stochastic forcing with fixed intermediate noise level, this translates into a larger Kramers rate, i.e. a higher

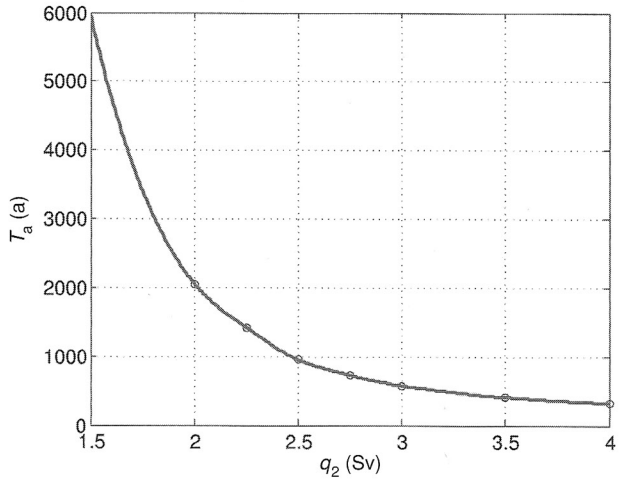

Figure 13.4 Average time interval T_a between two subsequent 'off'-to-'on'-switches in the conceptual stochastic model as a function of polar water inflow q_2. It is evident that a stronger polar water inflow to the Labrador Sea favours noise-induced transitions (i.e. reduction of the stochastic time scale). The values have been calculated from the Labrador Sea temperature time series (smoothed by a 70-year boxcar filter) of a 5×10^6-year integration.

frequency of switches between the two states of convection. Apart from the noise level, the polar water inflow q_2 is therefore the most efficient parameter to control the time scale of the oscillations in our conceptual model. Even relatively small changes in q_2 have a substantial effect on the stochastic time scale. For instance, the average time interval T_a between two subsequent 'off'-to-'on'-switches is about 2000 years for our standard set-up with $q_2 = 2$ Sv, and reduces to *c.* 1500 years for $q_2 = 2.25$ Sv and 750 years for $q_2 = 2.75$ Sv (Fig. 13.4). We therefore suggest that an increase in the flux of polar water from the Greenland Sea towards the Labrador Sea led to the mid-Holocene mode shift in North Atlantic climate variability towards a smaller period.

Indeed, there are indications from general circulation modelling that the supply of polar water from the Greenland Sea to the Labrador Sea was weaker in the early/mid Holocene than during the late Holocene. Climate simulations with the global coupled atmosphere–ocean model ECHO-G forced by varying orbital parameters show strong westerly wind anomalies over the North Atlantic between ~45° N and ~65° N during the early/mid Holocene (Lohmann *et al.* 2005). The stronger-than-present westerlies tended to block the westward flow of polar water from the East Greenland Current around the southern tip of Greenland and favoured a flow of polar water from the Greenland Sea towards the location

of sediment core LO09-14 southwest of Iceland. The ECHO-G model result is consistent with LO09–14's diatom record which shows that the Greenland Current assemblage was most influential during the early/mid Holocene.

As in ECBilt-CLIO, the noise-induced hopping between the 'on' and 'off' states in the conceptual model can be phase-locked to a sub-threshold periodic external forcing. According to stochastic resonance theory, the statistical synchronisation is strongest when the average waiting time between two noise-induced state transitions is comparable with half the period of the external forcing, i.e. when T_a approximately equals the forcing period (Gammaitoni *et al.* 1998). In other words, stochastic resonance requires the matching of two time scales: the deterministic time scale and the stochastic time scale (see also Chapters 7 and 11).

Given that the stochastic time scale can efficiently be modulated by the polar water influx q_2, the time scale matching condition for a prescribed forcing can be fulfilled by varying this parameter. This is demonstrated in Fig. 13.5, where frequency distributions of the time interval T (defined as the time interval between two subsequent 'off'-to-'on'-switches) are plotted for $q_2 = 2.25$ Sv and $q_2 = 2.75$ Sv. Without any external periodic forcing, a wide range of transition times is likely (Fig. 13.5, upper panel). Both distributions have a positive skew with an exponential shape that is characteristic for stochastic transitions driven by noise alone. The skew (and hence the dispersion of T) is more pronounced in the distribution with smaller q_2, reflecting the longer stochastic time scale in the experiment with $q_2 = 2.25$ Sv ($T_a \cong 1500$ years) compared to the case with $q_2 = 2.75$ Sv ($T_a \cong 750$ years).

We now apply sub-threshold sinusoidal forcings to the system. Sub-threshold means that the amplitude of the forcing is smaller than half the width of the hysteresis loop of the deterministic model (Fig. 13.2). In other words, the sinusoidal forcing alone (i.e. without the help of stochastic perturbations) is unable to induce a state transition from the 'off' mode to the 'on' mode or vice versa. A simple deterministic response to the sinusoidal forcing (albeit obscured by the noise) is therefore excluded.

When a small (3 mSv amplitude) sinusoidal forcing with a 750-year period is applied to the experiment with $q_2 = 2.75$ Sv, the approximate matching of the deterministic and stochastic time scales leads to a strong resonance such that a sharp peak appears at $T = 750$ years in the frequency distribution (Fig. 13.5, middle panel). The resonance is weaker in the $q_2 = 2.25$ Sv case, where pronounced secondary peaks are visible at integer multiples of the forcing period due to frequent 'skipping' of the forcing beat. Such a distribution indicates that the system operates on the interval of resonance. However, the statistical synchronisation is not optimized.

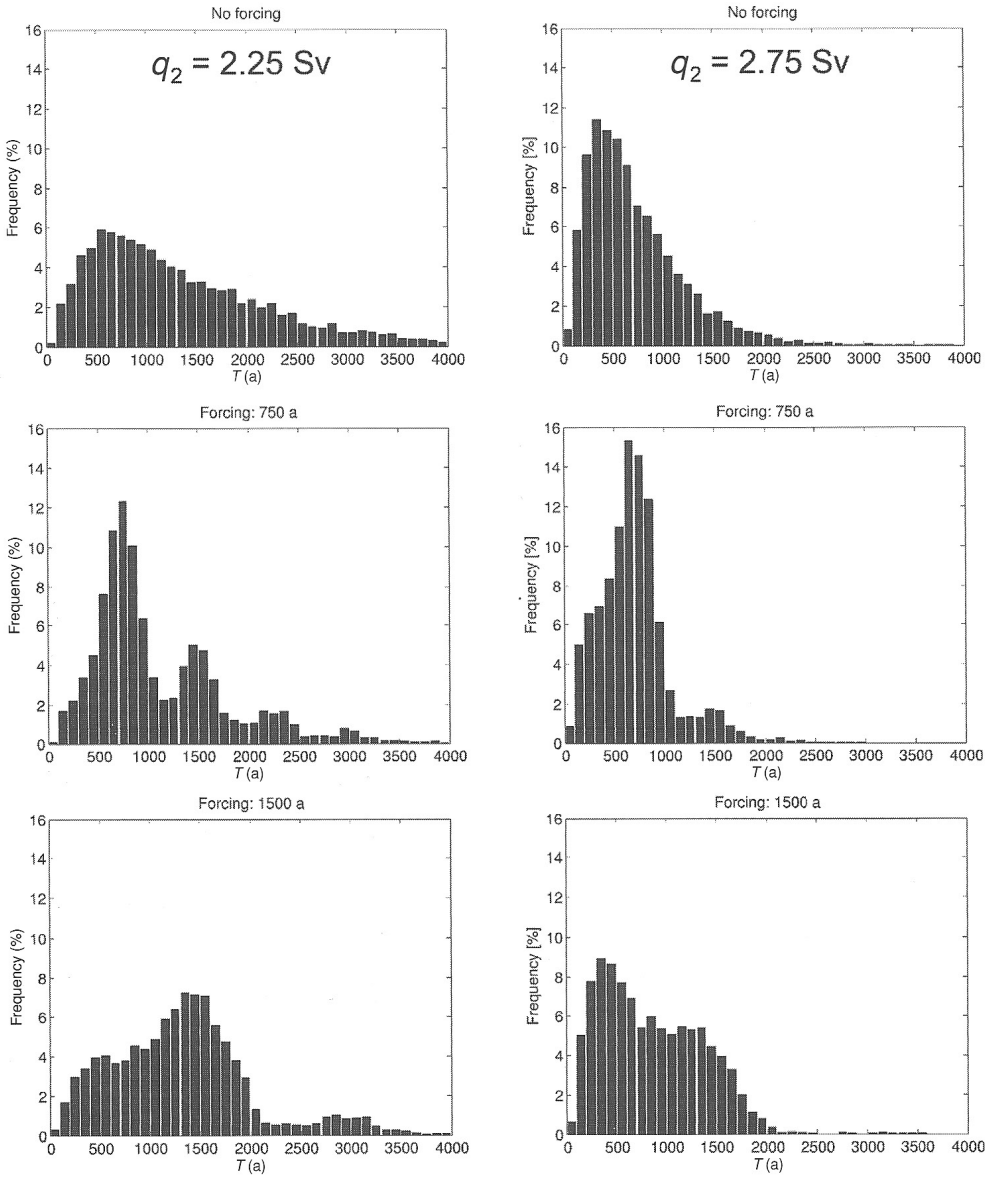

Figure 13.5 Frequency distributions of the time interval T (interval between two subsequent 'off'-to-'on'-switches) in the conceptual stochastic model for (left) $q_2 = 2.25$ Sv and (right) $q_2 = 2.75$ Sv. (Top) Without any external periodic forcing. (Centre) With sub-threshold (3 mSv amplitude) sinusoidal forcing of period 750 years. (Bottom) With sub-threshold (3 mSv amplitude) sinusoidal forcing of period 1500 years. The histograms are based on the Labrador Sea temperature time series (smoothed by a 70-year boxcar filter) of a 5×10^6-year integration.

The application of a forcing with 1500-year period (and again 3 mSv amplitude) leads to completely different results. The experiment with $q_2 = 2.75$ Sv does not show a statistical synchronisation with the sinusoidal forcing (Fig. 13.5, lower panel). Instead, the global maximum of the frequency distribution resides at the same location on the T-axis as in the unforced run. No maximum is found at 1500 years. By contrast, a maximum arises at 1500 years in the $q_2 = 2.25$ Sv experiment. While the noise-induced state switches in the $q_2 = 2.75$ Sv experiment are virtually 'immune' to the 1500-year forcing, a statistical synchronisation can be generated with $q_2 = 2.25$ Sv due to the longer stochastic time scale.

The subpolar SST record from core LO09-14 suggests a coupling to solar irradiance variations (Berner *et al.* 2008). We have shown that the noise-induced transitions between Labrador Sea convection 'on' and 'off' modes can indeed be phase-locked to a weak external forcing. The assumption that solar activity varies sinusoidally with one single period is however unrealistic. Instead, the power spectrum of solar irradiance reveals a multitude of superposed periods (Vonmoos 2005). We now examine how the noise-induced hopping with $q_2 = 2.25$ Sv and 2.75 Sv responds to a weak forcing that consists of two superposed sinusoids: one with a period of 750 years and the other one with a period of 1500 years. Both sinusoids have an amplitude of 3 mSv, hence the forcing remains sub-threshold (Fig. 13.6).

Figure 13.7 shows the frequency distributions of the time interval T for $q_2 = 2.25$ Sv and 2.75 Sv. In both cases, two prominent peaks are visible: one at 750 years and one at 1500 years (i.e. the time scales of the forcing). However, for $q_2 = 2.25$ Sv the global maximum is located at $T = 1500$ years, while it resides at 750 years in the $q_2 = 2.75$ Sv experiment. Although the forcing does not change between the two experiments, the structure of the frequency distribution does. With polar water inflow q_2 increasing from 2.25 Sv to 2.75 Sv, phase-locking to the 750-year mode of the forcing becomes more likely, while the 1500-year forcing becomes obscured.

In summary, we have shown that the stochastic switches between Labrador Sea convection 'on' and 'off' modes can be statistically synchronised with a weak external forcing that consists of different superposed sinusoids. In agreement with the theory of stochastic resonance, the strongest phase-locking occurs with that period in the forcing that is closest to the stochastic time scale of the noise-induced state transitions. We suggest that an increase in the polar water inflow during the mid Holocene led to a decrease of the stochastic time scale, thus favouring a synchronisation with a smaller period in the external (solar) forcing. This resulted in the 'observed' mid-Holocene mode shift of North Atlantic climate variability from ~1500 years in the early Holocene to 600–1000 years in the late Holocene.

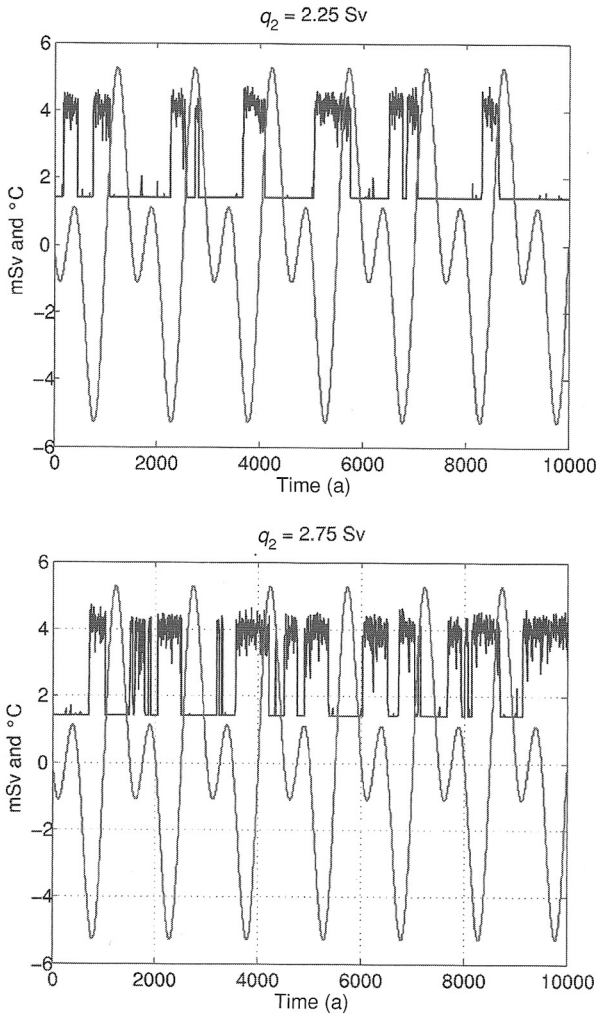

Figure 13.6 Typical time series of Labrador Sea temperature θ in the conceptual stochastic model with a weak (sub-threshold) forcing that consists of two superposed sinusoids (750 years and 1500 years; both sinusoids have an amplitude of 3 mSv) and a polar water inflow of (top) $q_2 = 2.25$ Sv and (bottom) $q_2 = 2.75$ Sv.

13.6 Discussion and conclusions

Centennial-to-millennial-scale North Atlantic climate variability in the coupled atmosphere–ocean model of intermediate complexity ECBilt–CLIO has been analysed (Schulz *et al.* 2007). The model exhibits internal oscillations of the AMOC that are characterised by a strong state with deep-water formation in both the Nordic seas

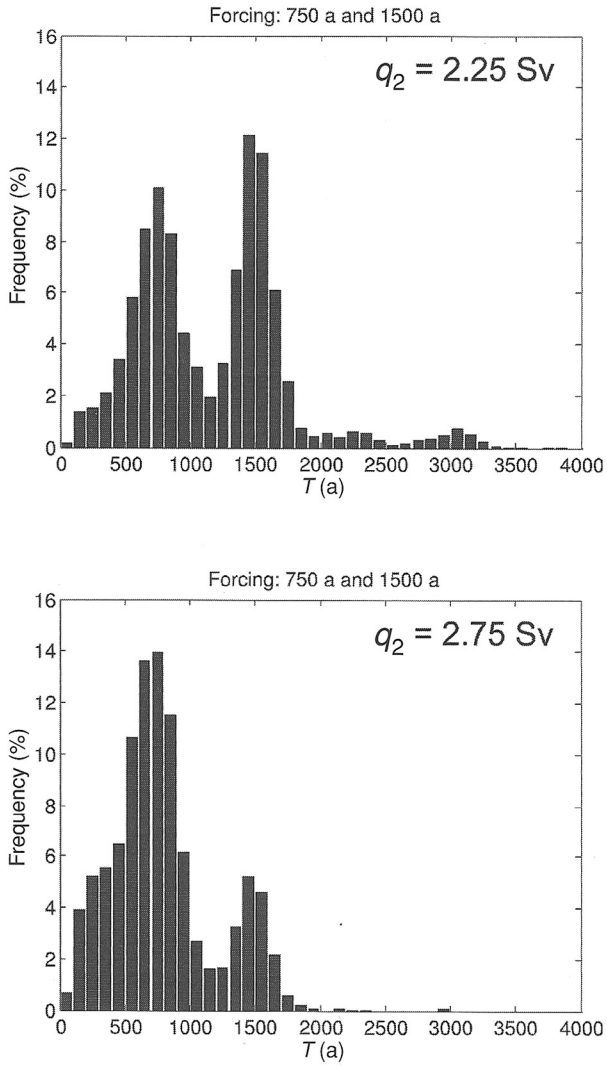

Figure 13.7 Frequency distributions of the time interval T (interval between two subsequent 'off'-to-'on'-switches) for (top) $q_2 = 2.25$ Sv and (bottom) $q_2 = 2.75$ Sv. A weak (sub-threshold) forcing that consists of two superposed sinusoids (periods of 750 and 1500 years) is applied (see Fig. 13.6).

and the Labrador Sea and a weak state in which deep water forms only in the Nordic seas. These oscillations can be attributed to an underlying bistability in Labrador Sea convection and state transitions induced by noise. In order to shift the system into the bistable regime, a small constant freshwater perturbation was applied to the Labrador Sea. The need for such a perturbation might be model-dependent. We note,

however, that other modelling studies (cf. Kuhlbrodt *et al.* 2001; Wood *et al.* 1999) suggest that the Labrador Sea operates close to the border of the bistable regime.

Temperature fluctuations associated with the AMOC oscillations in the North Atlantic are consistent with reconstructions from the Holocene, while they are much smaller compared to variations associated with glacial Dansgaard–Oeschger events (e.g. Voelker *et al.* 2002). A palaeoceanographic reconstruction for the Labrador Sea suggests changes in deep convection and a state-switching behaviour on centennial-to-millennial time scales since at least ~8000–9000 years before present (Hillaire-Marcel *et al.* 2001). Even though the resolution of the record is insufficient to capture the variability in Labrador Sea deep-water formation found in the model, the data suggest nearly a dozen state-switches during the Holocene. The magnitudes of the corresponding surface salinity and density variations in the Labrador Sea are similar to the changes accompanying a state-shift in the climate model.

A simple nonlinear stochastic model reproduces the centennial-to-millennial-scale oscillations observed in ECBilt-CLIO and highlights the important role of polar water flow towards the Labrador Sea in setting the stochastic time scale. In both the conceptual model and in ECBilt-CLIO the noise-induced transitions can be synchronised with a weak (sub-threshold) centennial-to-millennial-scale external forcing. It has thus been demonstrated that phase-locked switches in Labrador Sea convection can provide an amplifying mechanism for relatively weak climate perturbations. Hence, the model results support the hypothesis (Bond *et al.* 2001) on the existence of a centennial-to-millennial-scale amplifying mechanism involving ocean–atmosphere interactions that can operate under Holocene boundary conditions. The amplification of the weak external forcing depends on the presence of noise. The results suggest a stochastic resonance mechanism that can operate under Holocene conditions and indicate that changes in the three-dimensional configuration of NADW formation can be an important component of centennial-to-millennial climate variability during interglacials. By contrast, stochastic resonance on the millennial Dansgaard–Oeschger time scale was demonstrated for glacial boundary conditions by Ganopolski & Rahmstorf (2002). However, the two-dimensional zonally averaged Atlantic Ocean in their climate model did not exhibit noise-induced transitions and stochastic resonance under Holocene conditions. We therefore conclude that a three-dimensional model set-up, which is capable of simulating NADW formation in both the Nordic seas and in the Labrador Sea, is crucial for modelling interglacial AMOC oscillations.

Finally, we have presented a new hypothesis in an attempt to explain an observed mid-Holocene mode shift in the power spectrum of North Atlantic SST variability from ~1500 to 600–1000 years (Berner *et al.* 2008). This hypothesis involves a mid-Holocene increase of polar water flow from the Greenland Sea into the Labrador

Sea. The resulting decrease of the stochastic time scale favoured the phase-locking to a smaller period in the multimodal external forcing, in accordance with stochastic resonance theory.

Even though the phase-locking to an external forcing in the ECBilt-CLIO and conceptual model experiments is an important step towards understanding the relation between solar forcing and climate variability, it is still unclear how variations in solar irradiance translate into climate forcing. Ganopolski and Rahmstorf (2002), Schulz *et al.* (2007), and Jongma *et al.* (2007) implemented the external forcing through freshwater perturbations. We note that there is no evidence for a strong effect of solar irradiance variability on the hydrologic cycle; subtle fluctuations, however, cannot be ruled out. Another open question concerns the periodicities involved in solar variability. The periods used here and in the study of Jongma *et al.* (2007), i.e. 500, 750 and 1500 years, were chosen rather arbitrarily with the only goal to investigate whether the noise-induced AMOC transitions are susceptible to multicentennial and millennial external forcings. There is, however, evidence from cosmogenic isotope records that the solar power spectrum includes multicentennial periods (Bond *et al.* 2001; Vonmoos, 2005). In addition, Braun *et al.* (2005) suggested that millennial-scale solar forcing may arise through the superposition of 87- and 210-year solar cycles.

In future studies, experiments with other three-dimensional climate models, specifically more comprehensive models, should be carried out, to test the robustness of the mechanism that gives rise to the low-frequency AMOC oscillations in the climate model of intermediate complexity. The approach, however, is not straightforward. Firstly, a fine-tuning of the comprehensive models might be necessary in order to shift Labrador Sea convection into a bistable regime. Secondly, an integration of 10 000 years or more with a comprehensive climate model requires enormous computational resources. The acceleration technique employed by Lohmann *et al.* (2005) to make the long-term integration feasible inhibits the simulation of low-frequency climate variability.

We finally note that the understanding of low-frequency oscillations of Holocene climate is not only of importance from a palaeoclimatic perspective. It is also essential to understand the origin and dynamics of these natural climate variations to predict their potential interference with the possible anthropogenic influence on climate.

Acknowledgements

This work was funded through the DFG Research Centre / Excellence Cluster 'The Ocean in the Earth System'.

References

Benzi, R., Sutera, A. & Vulpiani, A. 1981 The mechanism of stochastic resonance, *J. Phys. A Math. Gen.*, **14**, L453–L457.

Berner, K. S., Koç, N., Divine, D., Godtliebsen, F. & Moros, M. 2008 A decadal-scale Holocene sea surface temperature record from the subpolar North Atlantic constructed using diatoms and statistics and its relation to other climate parameters. *Paleoceanography*, **23**, PA2210 (doi:10.1029/2006PA001339).

Bianchi, G. G. & McCave, I. N. 1999 Holocene periodicity in North Atlantic climate and deep-ocean flow south of Iceland. *Nature*, **397**, 515–517.

Bond, G., Showers, W., Cheseby, M. *et al.* 1997 A pervasive millennial-scale cycle in North Atlantic Holocene and glacial climates. *Science*, **278**, 1257–1266.

Bond, G., Kromer, B., Beer, J. *et al.* 2001 Persistent solar influence on North Atlantic climate during the Holocene. *Science*, **294**, 2130–2136.

Braun, H., Christl, M., Rahmstorf, S. *et al.* 2005 Possible solar origin of the 1,470-year glacial climate cycle demonstrated in a coupled model. *Nature*, **438**, 208–211.

Cessi, P. 1994 A simple box model of stochastically forced thermohaline flow. *J. Phys. Oceanogr.*, **24**, 1911–1920.

Dahl-Jensen, D., Mosegaard, K., Gundestrup, N. *et al.* 1998 Past temperatures directly from the Greenland ice sheet. *Science*, **282**, 268–271.

Dietrich, G., Kalle, K., Krauss, W. & Siedler, G. 1975 *Allgemeine Meereskunde.* Gebr. Borntraeger.

Freidlin, M. I. 2000 Quasi-deterministic approximation, metastability and stochastic resonance. *Phys. D*, **137**, 333–352.

Freidlin, M. & Wentzell, A. D. 1998 *Random Perturbations of Dynamical Systems*. Springer-Verlag.

Gammaitoni, L., Haenggi, P., Jung, P. & Marchesoni, F. 1998 Stochastic resonance. *Rev. Mod. Phys.*, **70**, 223–287.

Ganopolski, A. & Rahmstorf, S. 2002 Abrupt glacial climate changes due to stochastic resonance. *Phys. Rev. Lett.*, **88**, 038501 (doi:10.1103/PhysRevLett.88.038501).

Gent, P. R. & McWilliams, J. C. 1990 Isopycnal mixing in ocean circulation models. *J. Phys. Oceanogr.*, **20**, 150–155.

Goosse, H. & Fichefet, T. 1999 Importance of ice–ocean interactions for the global ocean circulation: A model study. *J. Geophys. Res.*, **C104**, 23337–23355.

Grootes, P. M. & Stuiver, M. 1997 Oxygen 18/16 variability in Greenland snow and ice with 10^{-3}- to 10^{5}-year time resolution. *J. Geophys. Res.*, **C102**, 26455–26470.

Hall, I. R., Bianchi, G. G. & Evans, J. R. 2004 Centennial to millennial scale Holocene climate – deep water linkage in the North Atlantic. *Q. Sci. Rev.*, **23**, 1529–1536.

Herrmann, S. & Imkeller, P. 2005 The exit problem for diffusions with time – periodic drift and stochastic resonance. *Ann. Appl. Probab.*, **15**, 39–68.

Hillaire-Marcel, C., de Vernal, A., Bilodeau, G. & Weaver, A. J. 2001 Absence of deep-water formation in the Labrador Sea during the last interglacial period. *Nature*, **410**, 1073–1077.

Jongma, J. I., Prange, M., Renssen, H. & Schulz, M. 2007 Amplification of Holocene multicentennial climate forcing by mode transitions in North Atlantic overturning circulation. *Geophys. Res. Lett.*, **34**, L15706 (doi:10.1029/2007GL030642).

Kloeden, P. E. & Platen, E. 1992 *Numerical Solution of Stochastic Differential Equations*. Springer-Verlag.

Kuhlbrodt, T., Titz, S., Feudel, U. & Rahmstorf, S. 2001 A simple model of seasonal open ocean convection. Part II: Labrador Sea stability and stochastic forcing. *Ocean Dyn.*, **52**, 36–49.

Lohmann, G., Lorenz, S. & Prange, M. 2005 Northern high-latitude climate changes during the Holocene as simulated by circulation models. In *The Nordic Seas: An Integrated Perspective*, Geophysical Monograph 158, ed. H. Drange, T. Dokken, T. Furevik, R. Gerdes and W. Berger, pp. 273–288. American Geophysical Union.

Monahan, A. H. 2002 Stabilisation of climate regimes by noise in a simple model of the thermohaline circulation. *J. Phys. Oceanogr.*, **32**, 2072–2085.

Nicolis, C. & Nicolis, G. 1981 Stochastic aspects of climatic transitions: additive fluctuations. *Tellus*, **33**, 225–234.

O'Brien, S. R., Mayewski, P. A., Meeker, L. D. *et al.* 1995 Complexity of Holocene climate as reconstructed from a Greenland ice core. *Science*, **270**, 1962–1964.

Oppo, D. W., McManus, J. F. & Cullen, J. L. 2003 Deepwater variability in the Holocene epoch. *Nature*, **422**, 277–278.

Opsteegh, J. D., Haarsma, R. J., Selten, F. M. & Kattenberg, A. 1998 ECBilt: a dynamic alternative to mixed boundary conditions in ocean models. *Tellus*, **50A**, 348–367.

Rind, D. 2002 The Sun's role in climate variations. *Science*, **296**, 673–677.

Schulz, M. & Paul, A. 2002 Holocene climate variability on centennial-to-millennial time scales: 1. Climate records from the North-Atlantic realm. In *Climate Development and History of the North Atlantic Realm*, ed. G. Wefer, W. H. Berger, K.-E. Behre and E. Jansen, pp. 41–54. Springer-Verlag.

Schulz, M., Prange, M. & Klocker, A. 2007 Low-frequency oscillations of the Atlantic Ocean meridional overturning circulation in a coupled climate model. *Clim. Past*, **3**, 97–107.

Stastna, M. & Peltier, W. R. 2007 On box models of the North Atlantic thermohaline circulation: intrinsic and extrinsic millennial timescale variability in response to deterministic and stochastic forcing. *J. Geophys. Res.*, **112**, C10023 (doi:10.1029/2006JC003938).

Stommel, H. 1961 Thermohaline convection with two stable regimes of flow. *Tellus*, **13**, 224–228.

Stommel, H. & Young, W. 1993 The average T–S relation of a stochastically-forced box model. *J. Phys. Oceanogr.*, **23**, 151–158.

Voelker, A. H. L. and workshop participants 2002 Global distribution of centennial-scale records for Marine Isotope Stage (MIS) 3: a database. *Q. Sci. Rev.*, **21**, 1185–1212.

Vonmoos, M. 2005 Rekonstruktion der solaren Aktivität im Holozän mittels Beryllium-10 im GRIP Eisbohrkern. Ph.D. Thesis, ETH Zürich, Switzerland.

Wood, R., Keen, A., Mitchell, J. & Gregory, J. 1999 Changing spatial structure of the thermohaline circulation in response to atmospheric CO_2 forcing in a climate model. *Nature*, **399**, 572–575.